Controllable band structure in a periodic quantum well

Victor A. Pogrebnyak*
Department of Electrical and Electronics Engineering, Faculty of Engineering and Architecture, Çukurova University, Adana 01330, Turkey

(Received 8 October 2003; revised manuscript received 10 March 2004; published 15 June 2004)

Electron states in a two-dimensional (2D) infinitely deep quantum well, having periodically corrugated walls, are analyzed. It is shown that corrugation causes resonant interaction between the transverse modes of the electron wave function. The interaction results in the non-Bragg nature electron resonances, which give rise to opening of additional band gaps, besides usual Bragg gaps. The position of the non-Bragg and Bragg gaps in the quantum-well band structure depends on a period of corrugation and thickness of the quantum well. For example, for a change in average thickness or period, at some of its value, one of the 2D levels becomes resonant, and it causes the level splitting and the creation of a 2D subband with the negative effective mass. The values of the effective mass and gap width depend also on the phase shift between two periodic boundaries. These quantities vary from zero to a maximum value upon shifting of one periodic boundary with respect to another on the half period of corrugation. In the well having the congruent periodic boundaries, there are no Bragg gaps in the band structure. The lateral periodicity causes the anisotropic stripelike electron-density distribution in such a periodic quantum well.

DOI: 10.1103/PhysRevB.69.245307 PACS number(s): 73.21.Fg, 73.21.Ac

I. INTRODUCTION

The study of two-dimensional electronic systems evokes considerable interest due to the broad utilization of the systems in microelectronics[1–4] as well as for the close relation of this problem to explanation of high-temperature superconductivity.[5–6] Design of new devices are commonly based on exploiting the different configurations of multiple-quantum-well structures and superlattices. Technological advances in this field allow enable the tailoring of electronic properties of the nanostructures by varying of parameters of quantum wells and barriers.[3–9] In these nanostructures, the vertical transport of electrons across quantum wells is commonly used. Despite great progress in this field, a multiple quantum well (MQW) has one main inherent defect: a period of the structure is always greater than a thickness of a single-quantum well. Therefore, the electron energy, associated with the period, is always less than the energy of the ground state in the single-quantum well. Taking into consideration that the energy level crossing causes important resonance properties of the system, it becomes clear that these resonant properties are excluded from MQW structures using the vertical transport. This defect can be avoided if the in-plane transport of electrons in a quantum well with periodic boundaries is used. In this case there are neither physical nor principal technological[3,10–12] restrictions on the relationship between thickness and a period. Moreover, modern technology can create the bias voltage tunable lateral modulation using the same principle as in the metal-oxide-semiconductor transistor.[3]

Similar problems arise in the investigation of a two-dimensional electron gas (2DEG) in 2D layered structures, copper-oxide ceramics, at the boundary of a heterostructure or at grain boundaries in mosaic crystals. In these cases a lateral modulation can be caused by the crystal lattice or by the presence of a plane array of dislocations, which form a one- or two-dimensional long-period lateral modulation.[13–15] It appears necessary, then, to analyze electron states in a quantum well having periodic boundaries in the free electron approximation. In spite of the fact that 2D electron systems are studied in detail, the periodic quantum well did not attract much attention. In 2DEG problems, the periodic crystal potential was usually included into the effective mass, as a 3D potential, but not as a 2D lateral modulation potential. To our knowledge, the quantum-well band structure caused by periodic lateral modulation, the effect of the phase shift between two periodic boundaries on the band structure, and the effective mass of an electron have not been studied. These problems can be solved analytically by using the standard perturbation theory. As a result, as shown in the paper, new fundamental properties of a 2DEG are revealed in such a periodic quantum well.

In Ref. 16 it is shown that the periodic quantum-well band structure essentially changes if the characteristics energies corresponding to the transverse and longitudinal electron motion become equal. The analysis, presented in this communication, shows that the lateral modulation results in the opening of additional gaps and in the creation the subband with the negative effective mass. As a result the sharp anisotropy of the effective-mass and transport phenomena, for electron motion perpendicular and parallel to grooves, arises in such a periodic quantum well.

II. INITIAL EQUATIONS

Consider an infinitely deep potential well of thickness d, where both walls have one-dimensional periodic corrugations described by the functions $y_{-d}(x) = -d/2 + \xi \cos(qx)$ for the left boundary and $y_d(x) = d/2 + \rho \cos(qx + \theta)$ for the right boundary, where $q = 2\pi/a$; ξ, ρ, and a are amplitudes and a period of the corrugations, the parameter θ is the phase shift between the right and left periodic corrugations. As we mentioned before, a may have a value of the crystal lattice constant or any other value depending on a periodic profile

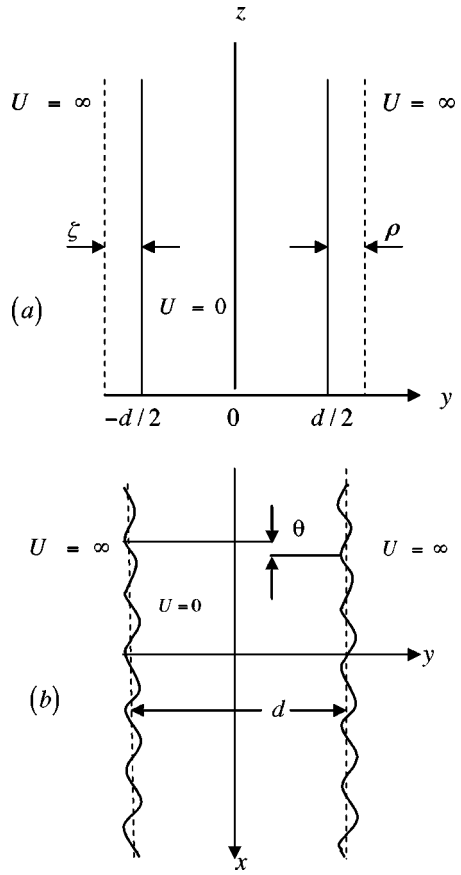

FIG. 1. Two-dimensional potential-energy profile of a periodically corrugated quantum well is shown in the zy plane (a) and a lateral profile in the xy plane (b); θ is the phase shift between the left and right periodic boundaries.

of the boundary. Thus, an electron is in a well bounded by a two-dimensional potential $U(x,y)$

$$U(x,y)=\begin{cases} 0 & -d/2<y<d/2 \\ \infty & y_d(x)\leqslant y\leqslant y_{-d}(x) \end{cases}. \tag{1}$$

This potential pattern is illustrated in Fig. 1.

The wave function $\psi(x,y,z)$ and the energy of the electron are found by solving the three-dimensional stationary Schrodinger equation

$$-\frac{\hbar^2}{2m}\left(\frac{\partial^2}{\partial x^2}+\frac{\partial^2}{\partial y^2}+\frac{\partial^2}{\partial z^2}\right)\psi+U(x,y)\psi=E\psi, \tag{2}$$

subject to the boundary condition

$$\psi(x,y_{-d}(x),z)=\psi(x,y_d(x),z)=0, \tag{3}$$

where E is the electron energy, m is the mass of the free electron. Due to the boundary periodicity, $\psi(x,y,z)$ can be represented in the form of a Fourier series (Floquet's theorem)

$$\psi(x,y)=\sum_n\ [a_n\cos(k_{yn}y)+b_n\sin(k_{yn}y)]\times\exp[j(k_x+nq)x+jk_zz], \tag{4}$$

where a_n and b_n are the Fourier series coefficients, k_{yn} and k_x, k_z are the transverse and longitudinal components of the wave vector $\mathbf{k}$.

From the Schrodinger equation and Eq. (4) follows the dispersion relation $E(k)$:

$$E=\frac{\hbar^2(k_x+nq)^2}{2m}+\frac{\hbar^2k_{yn}^2}{2m}+\frac{\hbar^2k_z^2}{2m}. \tag{5}$$

Substitution of Eq. (4) into the boundary condition gives a system of linear algebraic equations for the coefficients a_n and b_n. By equating to zero the determinant of this system, the allowed values of k_{yn} can be found. Hence, the dispersion relation in the quantum well is determined. For small corrugations, $\xi/d\ll1$, $\rho/d\ll1$ and $\xi q\ll1$, $\rho q\ll1$, it is sufficient to retain the first three space harmonics. As a result, the following characteristic equation is obtained for determination of allowed values of k_{y0},

$$\tan(k_0d)=\frac{1}{4}(\xi^2+\rho^2)\left\{\frac{k_0k_1}{\tan(dk_1)}+\frac{k_0k_{-1}}{\tan(dk_{-1})}\right\}-\frac{1}{2}\xi\rho\frac{\cos\theta}{\cos(k_0d)}\left\{\frac{k_0k_1}{\sin(k_1d)}+\frac{k_0k_{-1}}{\sin(k_{-1}d)}\right\}, \tag{6}$$

where $k_{\pm1}$ are the wave numbers of the $n=\pm1$ harmonics

$$k_{\pm1}=\sqrt{k_0^2\mp2k_xq-q^2}. \tag{7}$$

In Eq. (6), Eq. (7) and below the subscript y is dropped in the wave numbers k_{yn}.

III. SHIFT OF THE 2D LEVELS

The solution of Eq. (6) is sought by the method of successive approximation with respect to ξ and ρ, i.e., $k_0=k_0^{(0)}+\delta k+\cdots$. In a case of smooth boundaries, $\xi=0$ and $\rho=0$, Eq. (6) gives $\tan(k_0^{(0)}d)=0$. Therefore,

$$k_0^{(0)}=\frac{p\pi}{d}\equiv k_{0p},\quad p=1,2,3,...,$$

$$E=E_{0p}+\frac{\hbar^2(k_x^2+k_z^2)}{2m},\quad E_{0p}=\frac{\hbar^2p^2\pi^2}{2md^2}. \tag{8}$$

These are well-known 2D subbands in a smooth quantum well.

In the next approximation, for $\xi\neq0$ and $\rho\neq0$, the 2D levels E_p and their shifts δE_p with respect to location in the smooth quantum well are

$$E_p=\left[1+\frac{\xi^2+\rho^2}{2d}k_1\cot(k_1d)+(-1)^{p+1}\frac{\xi\rho k_1\cos\theta}{2d\sin(k_1d)}\right]E_{0p}, \tag{9}$$

$$\delta E_p=\left[\frac{\xi^2+\rho^2}{2d}k_1\cot(k_1d)+(-1)^{p+1}\frac{\xi\rho k_1\cos\theta}{2d\sin(k_1d)}\right]E_{0p}. \tag{10}$$

Equation (9) describes a location of the 2D levels as a function of the geometric parameters ξ,ρ,d, and a. Formulas (6) and (9) are counterparts of Eq. (8) for the smooth quantum well. The last two equations and Eq. (6) indicate the nontrivial dependence of E_p on the $k_{\pm 1}$ wave numbers and on geometric dimensions of the quantum well. Primarily it displays the resonance behavior of the system, but of not less importance is the dependence of E_p on an angle θ, i.e., a dependence on the phase shift of one periodic boundary with respect to another. As will be seen below, both dependencies cause new fundamental properties of electron behavior in the periodic quantum well.

IV. NON-BRAGG RESONANCES

It is seen from Eqs. (6), (9), and (10) that resonance in the system occurs if

$$k_{\pm 1}=\sqrt{k_0^2 \mp 2k_x q-q^2}=\frac{r\pi}{d}\equiv k_{1r}, \quad r=1,2,3,.... \quad (11)$$

The new quantum number r designates the order number of the resonance in the system. From Eq. (11), it is seen that $r\leqslant p$ in the first Brillouin zone. The Bragg resonance, $k_x^{\pm}=\pm q/2$, is a particular case of Eq. (11) at $r=p$. Equation (11) along with Eq. (9) are condition of the non-Bragg resonance between transverse modes of the wave function, and it can be written in the form

$$k_{\pm 1}=\frac{r\pi}{d}\equiv k_{1r}, \quad k_{0p}=\frac{p\pi}{d}. \quad (12)$$

The physical meaning of the resonance condition becomes clear if the last equations are rewritten in terms of the de Broglie wavelength ($\lambda=2\pi/k$) associated with the transverse modes ($k_0^{(0)}$ and $k_{\pm 1}$) of the fundamental ($n=0$) and the $n=\pm 1$ space harmonics of the electron wave function

$$d=p\frac{\lambda_0}{2}=r\frac{\lambda_1}{2}. \quad (13)$$

Equation (13) shows that a resonance arises if the thickness of the well d is simultaneously a multiple of the de Broglie half wavelengths associated with transverse modes of the fundamental ($n=0$) and $n=\pm 1$ space harmonics but with different quantum numbers p and r Schematic illustration of this phenomenon is given in Fig. 2.

It is appropriate to underline here that in contrast to common consideration of interference of electronic traveling waves that gives rise to the Bragg gap, Eqs. (12) and (13) are the condition of the constructive or destructive interference of electronic standing waves (transverse modes). That is why this resonance is of a non-Bragg nature.

The resonant value $k_{x,p,r}^{\pm}$ of the wave number k_x, at which the resonance condition (13) holds, can be found from Eq. (11)

$$k_{x,p,r}^{\pm}=\pm\frac{1}{2q}(k_{0p}^2-q^2-k_{1r}^2). \quad (14)$$

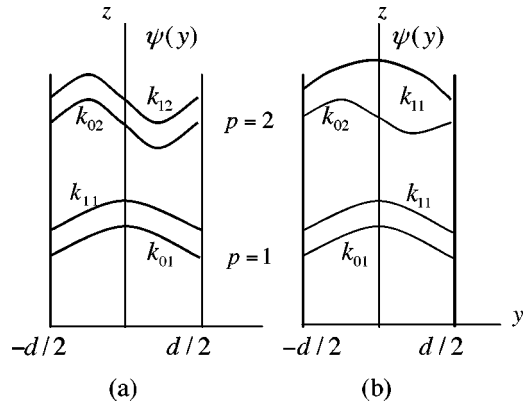

FIG. 2. Variation of the fundamental (k_{op}) and first space (k_{1r}) harmonics of electron wave function $\psi(y)$ with the y coordinate for the ground, $p=1$, and the first exited, $p=2$, energy states. k_{op} and k_{1r} are wave numbers of transverse modes, Eq. (12). (a) In a case of Bragg resonances, the wave functions have always similar wave forms. (b) Wave forms of transverse modes, having k_{02} and k_{11} wave numbers, are different. This is the non-Bragg resonance.

The upper sign "+" is taken for the resonant $n=1$ harmonic and the lower "minus"—for the $n=-1$ harmonic. In Eq. (14) it is enough to consider the range $k_x>0$ since it is obviously that $k_{+1}(-|k_x|)=k_{-1}(|k_x|)$.

The wave functions of electrons with the resonant k_x have the standing wave wave form along the x-axis, but the electrons can move freely in the transverse direction. This anisotropy of electron motion resembles the stripe phase in high-temperature superconductors.

V. SUBMINIZONE SPECTRUM

Substitution of $k_{x,p,r}^{\pm}$ into Eq. (5) gives an expression for the resonant energy

$$E_{pr}=\frac{\hbar^2}{2m}\left\{k_{0p}^2+\left(\frac{k_{0p}^2-q^2-k_{1r}^2}{2q}\right)^2\right\}. \quad (15)$$

In vicinity of resonance, the more accurate solution of Eq. (6) shows that this resonant energy level splits into two values E_{pr}^{+} and E_{pr}^{-}, separated by the forbidden gap δE_{pr},

$$E_{pr}^{\pm}=E_{pr}\left\{1\pm\frac{E_{0p}}{E_{pr}}\frac{r}{p}\frac{1}{d}[\xi^2+2(-1)^{p+r+1}\xi\rho\cos\theta+\rho^2]^{1/2}\right\}, \quad (16)$$

$$\delta E_{pr}=E_{pr}^{+}-E_{pr}^{-}=2E_{0p}\frac{r}{p}\frac{1}{d}[\xi^2+2(-1)^{p+r+1}\xi\rho\cos\theta+\rho^2]^{1/2}. \quad (17)$$

Thus, the resonances divide the pth subband into subminizones. The quantum number r shows the order number of the subminizone in the subband. A number of subminizones in the minizone can be found from relation (11). Since the last gap (Bragg gap) takes place at $r=p$, it means that a number of subminizones equals the order number p of given

subband. The number of subminizones is the same as a number of gaps, including the Bragg gap. The range $k_{x,r}$ between two successive resonances in the k space can be found from Eq. (14):

$$k_{x,r}=k^{+}_{x,p,r+1}-k^{+}_{x,p,r}=\frac{2r+1}{2q}\frac{\pi^2}{d^2}. \tag{18}$$

It does not depend on the quantum number p.

A. The negative effective mass

From Eq. (15) it is seen that the resonant energy approaches to the ground state E_{0p} as the expression in the brackets $(k_{0p}^2-q^2-k_{1r}^2)$ vanishes. Equality of this expression to zero imposes relationship between the thickness d and the period a, and quantum numbers p and r

$$d_{res}=\frac{a}{2}\sqrt{p^2-r^2}. \tag{19}$$

It means that given 2D level will be resonant under the specific geometric relationship. That is why the resonance can be named as the geometric resonance in a periodic quantum well. By analogy with solutions (16) and (17), the 2D level of the pth subband E_{0p} splits at $d=d_{res}$, into two levels E^{+}_{pr} and E^{-}_{pr}, separated by the gap δE_{pr},

$$E^{\pm}_{pr}=\left[1\pm\frac{1}{d}\frac{r}{p}[\xi^2+2(-1)^{p+r+1}\xi\rho\cos\theta+\rho^2]^{1/2}\right]E_{0p}, \tag{20}$$

$$\delta E_{pr}=\frac{2}{d}\frac{r}{p}[\xi^2+2(-1)^{p+r+1}\xi\rho\cos\theta+\rho^2]^{1/2}E_{0p}. \tag{21}$$

Since δE_p is the forbidden gap, the geometric resonance causes the creation of the subminizone E_p^- with the negative effective mass

$$m^*=-\frac{1}{2\sqrt{2}}\frac{1}{d}[\xi^2+2(-1)^{p+r+1}\xi\rho\cos\theta+\rho^2]^{1/2}\frac{k_{0p}k_{1r}}{q^2}m. \tag{22}$$

From Eqs. (6)–(22) it is seen that the band structure and the effective mass of the electron in the quantum well substantially depend on the phase shift θ between two periodic boundaries.

VI. EFFECT OF THE PHASE SHIFT ON VALUES OF THE GAP AND THE EFFECTIVE MASS

In this section the dependence of width of the gap, Eq. (17), and the effective mass, Eq. (22), on the phase shift θ between two periodic boundaries is investigated. The analysis is given here for two cases: (1) $\theta=0$, which may be called as a case of asymmetric boundaries, and, (2) $\theta=\pi$, which corresponds to shifting of the right boundary on the half period of the corrugation. In the latter case the boundaries are symmetrical with respect to the centerline of the well—the x axis.

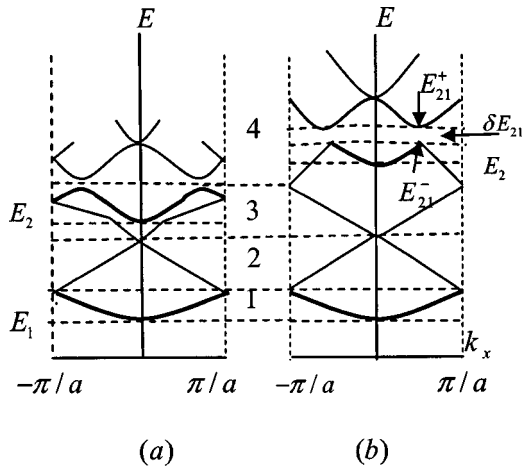

FIG. 3. Schematic representation of dispersion curves $E(k_x)$ for different relations between thickness d and period a in the asymmetric quantum well. (a) Energy level E_2 is located in the third minizone of the ground 2D subband. (b) Energy level E_2 is located in the fourth minizone.

A. Asymmetric well, $\theta=0$

In this case, if $\xi=\rho$, a separation between the congruent boundaries is constant and equal to d at any value of the x coordinate. If $\xi\neq\rho$, the deviation from d is equal to $\pm|\xi-\rho|$.

(a) If both p and r are even or both are odd numbers, the expressions (22), (16), and (17) for the effective mass, the resonant energy, and the gap take the form

$$m^*=-\frac{1}{2\sqrt{2}}\frac{|\xi-\rho|}{d}\frac{k_{0p}k_{1r}}{q^2}m, \tag{23}$$

$$E^{\pm}_{pr}=\left(1\pm\frac{|\xi-\rho|}{d}\frac{r}{p}\frac{E_{0p}}{E_{pr}}\right)E_{pr},\quad \delta E_{pr}=2\frac{r}{p}\frac{|\xi-\rho|}{d}E_{0p}. \tag{24}$$

(b) If p is even but r is odd or vice versa, then

$$m^*=-\frac{1}{2\sqrt{2}}\frac{(\xi+\rho)}{d}\frac{k_{0p}k_{1r}}{q^2}m, \tag{25}$$

$$E^{\pm}_{pr}=\left(1\pm\frac{(\xi+\rho)}{d}\frac{r}{p}\frac{E_{0p}}{E_{pr}}\right)E_{pr},\quad \delta E_{pr}=2\frac{r}{p}\frac{(\xi+\rho)}{d}E_{0p}. \tag{26}$$

Figure 3 shows qualitative representation of the dispersion curves $E(k_x)$ and split levels $E^{\pm}_{pr}$ for the first two 2D subbands in the asymmetric quantum well for different relations between thickness and period.

B. Symmetric well, $\theta=\pi$

In this case a separation between boundaries varies with the x coordinate between values $d+\xi+\rho$ and $d-\xi-\rho$.

(a) If both p and r are even or both are odd numbers, the expressions for the effective mass, split energy levels, and δE_{pr} are given by Eqs. (25) and (26).

(b) If p is even and r is an odd number or vice versa the result is the same as Eqs. (23) and (24).

From Eqs. (25) and (26) it is first seen that the gap δE_{pr} and m^* are proportional, as expected, to the perturbation $(\xi+\rho)/d$ caused by corrugations. But Eqs. (23) and (24) show that this common rule is not always valid. In the case of the asymmetric well, described by Eqs. (23) and (24), all Bragg gaps ($r=p$) and the effective mass vanish if $\xi=\rho$. Only the subminizone gaps, which have the order number r of different evenness than the quantum number p, remain in the energy spectrum of the subband. The widths of these gaps are defined by Eq. (26). Thus, in a quantum well having the congruent periodic boundaries, there are no Bragg gaps in the band structure.

In the symmetric well, the Bragg gaps as well as subminizone gaps have the maximum value given by Eq. (25). The effective mass and subminizone gaps, defined by the condition (6) above, vanish. Figure 4 presents illustration of such a transformation of dispersions for the first two 2D subbands upon phase shift θ in a quantum well with a specific configuration corresponding to the geometric resonance case.

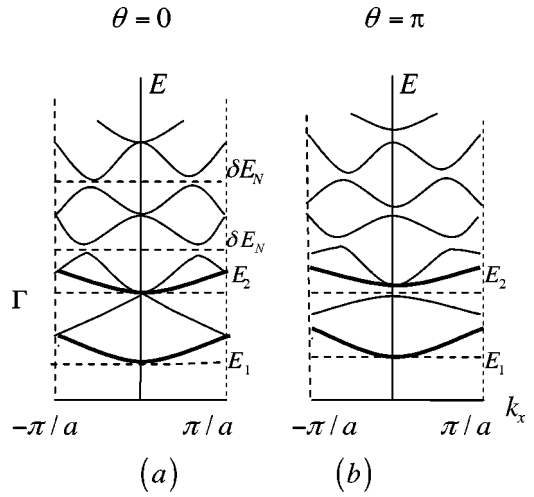

FIG. 4. Qualitative evolution of $E(k_x)$ vs phase shift θ. (a) Illustrates gapless zone folding in the asymmetric quantum well. There are no Bragg gaps at the edge and center of the first Brillouin zone. Only non-Brag gaps δE_N open due to the energy level crossing. (b) Upon phase shit $\theta=\pi$, in the symmetric well, Bragg gaps open and have maximum values. For this particular illustration, in both (a) and (b) cases, d and a are chosen to satisfy to the geometric resonance condition (19): the top of the second minizone touches the bottom of the second 2D subband (point Γ).

VII. EVALUATION

Let us estimate δE_{pr} for a periodic quantum well having parameters close to the experimental realization of such a structure in Ref. 11. Consider a thickness of the well $d=200$ Å, then a period of lateral modulation, a [see Eq. (19)], equals to 231 Å. Assume an amplitude of the modulation equal to 10% of d and take $m=0.058m_0$ (InGaAs). In this case, the band gap $\delta E_{21}=13$ meV opens in the vicinity of the second energy level E_2. The gap can be observed, for example, by measuring a dc conductivity in a direction perpendicular to grooves at helium temperatures. When the Fermi energy E_F coincides with the onset of δE_{21}, the conductivity significantly drops due to the gap. E_F can be changed by biasing or by doping as in cuprate superconductors or, vice versa, the location of δE_2 can be altered by varying d and a. In accordance with Eq. (25), anisotropy of the effective mass, $m^*(\perp)/m^*(\parallel)$, for electron motion perpendicular ($\perp$) and parallel ($\parallel$) to grooves, equals 5.55. These estimates are in qualitative agreement with the experimental results in Ref. 11. However, the geometry of the InGaAs periodic channel in Ref. 11 does not match the optimal dimensions taken here. The gap can be also detected by investigating the photoeffect at $\lambda=95.4$ μm.

In discussing properties of a 2DEG in semiconductors and metallic compounds, caused by a lateral periodic modulation, it is important to note the essential difference of the properties in these materials, which originated due to different values of the electron mean-free path in the media. The principal condition of observation of the properties, caused by periodicity, is $l \gg a$, where l is the electron mean-free path, and a is a period of the lateral modulation. In semiconductors the condition is usually met at helium temperatures, while for metal crystals, it can meet at much higher temperatures, up to the room temperature, depending on a value of a. This could be one of reasons of the observation of a large transport anisotropy only at low temperatures in semiconductors,[14,17,18] but at much higher temperatures in layered metallic crystal such as cuprates.

VIII. CONCLUSION

The investigation shows that the lateral periodic modulation of a 2DEG causes Bragg and non-Bragg resonances and gaps, which transform the band structure into subminizones. The Bragg gap corresponds to the last non-Bragg resonance ($p=r$) in the subminizone structure, and as usual, it is the gap at the boundary of the Brillouin zone. A number of gaps (the same as subminizones), including the Bragg gap, is equal to the order number of the subband. For example, there are two subminizones in the second subband ($p=2$).

At some specific configuration, the geometric resonance occurs in the periodic quantum well. This phenomenon consists of the crossing of the folded 2D levels at a certain relationship between a thickness and a period of the well. As a result, an electron state with the negative effective mass arises in the 2D subband. A width δE_{pr} of the gap and a value of the effective mass m^* depend on the phase shift θ between two periodic boundaries and evenness of quantum numbers p and r. δE_{pr} and m^* vary from zero to a maximum value upon shifting of one periodic boundary with respect to another on the half period of corrugation. In a well having the congruent periodic boundaries, Bragg gaps do not open. Unlike the effective-mass approximation, results (19)–(26) reveal anisotropy for electron motion perpendicular and parallel to grooves, caused by the lateral modulation.

After introducing a lateral periodic potential into a 2DEG, it becomes possible to transfer general properties of crystals, caused by 3D or 2D periodicity, to the case of the 2DEG. Recent theoretical and experimental achievements in the

study of two-dimensional photonic crystals, see, for example, Ref. 19, permits direct transfer of their properties to the 2DEG. A two-dimensional (square, hexagonal, etc.) lateral periodic modulation of a 2DEG in layered crystals, heterostructures, copper-oxide ceramics as well as at grain boundaries in mosaic crystals can be caused by the crystallographic potential or misfit dislocations.[13–15] Unlike a one-dimensional periodic modulation, Eq. (1), a strong 2D periodic modulation creates a real complete band gap for any **k**. In cuprates, parameters d and a are more than 20 times smaller than in the example given above (in effective-mass approximation), so the gap would be much greater and may match the Fermi level in the metallic state. If the Fermi level coincides with the gap, the 2DEG does not conduct current.

The transport properties of the 2DEG are largely determined by the shape of the Fermi surface. The anisotropy in the shape of the Fermi surface become quite sharp as it intersects boundaries of the Brillouin zones. For example, for a square lattice, formed by the lateral modulation, the Fermi surface has a almost square shape (holelike) in the second zone and starlike shape (electron type) in the third zone. The shape of the Fermi surface results in the anisotropy of the electron velocity, $\mathbf{v}=_k E(k)$, and transport phenomena in the 2DEG in the same manner as anisotropy of wave propagation occurs in photonic crystals. In Ref. 20, the anisotropy of light propagation in a hexagonal 2D photonic crystal was demonstrated; the angle between allowed directions equals 60°. In a laterally modulated 2DEG, such an anisotropy of electron motion results the stripelike electron-density distribution; electrons move along allowed directions and have a standing wave waveform distribution in transverse directions. Two such conducting wells (channels) connected in successive order form an insulating junction if their allowed directions are nonparallel to each other.

ACKNOWLEDGMENTS

This work was supported by the Scientific and Technical Research Council of Turkey (TUBITAK) through a Project No. 101E045.

*Email address: vpog@cu.edu.tr

[1] T. Ando, A.B. Fowler, and F. Stern, Rev. Mod. Phys. **54**, 437 (1982).

[2] C. Weisbuch and B. Vinter, *Quantum Semiconductor Structures: Fundamentals and Applications* (Academic Press, New York, 1991).

[3] M.J. Kelly, *Low-dimensional Semiconductors: Materials, Physics, Technology, Devices* (Clarendon Press, Oxford, 1995).

[4] A. Shik, *Quantum Wells: Physics and Electronics of Two-dimensional Systems* (World Scientific, Singapore, 1997).

[5] J.M. Tranquada, B.J. Sternlieb, J.D. Axe, Y. Nakamura, and S. Uchida, Nature (London) **375**, 561 (1995).

[6] V.J. Emery, S.A. Kivelson, and J.M. Tranquada, Proc. Natl. Acad. Sci. U.S.A. **96**, 8814 (1999).

[7] *Physics of Low Dimensional Semiconductor Structures*, edited by P. Butcher, N.H. March, and M.P. Tosi (Plenum Press, New York, 1993).

[8] K.K. Choi, C.J. Chen, and D.C. Tsui, J. Appl. Phys. **88**, 1612 (2000).

[9] A. Majumdar, K.K. Choi, L. Rokhinson, and D.C. Tsui, Appl. Phys. Lett. **80**, 538 (2002).

[10] P.M. Petroff *et al.*, J. Cryst. Growth **95**, 260 (1992).

[11] M. Akabori, J. Motohisa, and T. Fukui, Physica E **7**, 766 (2000).

[12] T. Fukui, K. Tsubaki, H. Saito, M. Kasu, and S. Honda, Surf. Sci. **267**, 588 (1992).

[13] V.A. Pogrebnyak, I.M. Rarenko, D.D. Khalameia, and V.M. Yakovenko, Fiz. Tekh. Poluprovodn. **32**, 319 (1998) [Semiconductors **32**, 288 (1998)].

[14] N.L. Bobrov, L.F. Rybal'chenko, V.V. Fisun, I.K. Yanson, O.A. Mironov, S.V. Chistyakov, V.V. Sorchenko, A.Yu. Sipatov, and A.I. Fedorenko, Fiz. Nizk. Temper. **16**, 1531 (1990) [Sov. J. Low Temp. Phys. **16**, 862 (1990)].

[15] H.F. Matare, *Defect Electronics in Semiconductors* (Wiley-Interscience, New York, 1971).

[16] V.A. Pogrebnyak, Fiz. Tver. Tela (St. Petersburg) **41**, 1867 (1999) [Phys. Solid State **41**, 1715 (1999)].

[17] M.P. Lilly, K.B. Cooper, J.P. Eisenstein, L.P. Pfeiffer, and K.N. West, Phys. Rev. Lett. **82**, 394 (1999).

[18] U. Zeitler, H.W. Schumacher, A.G.M. Jansen, and R.J. Haug, Phys. Rev. Lett. **86**, 866 (2001).

[19] *Photonic Crystal and Light Localization in the 21 Century*, edited by C.M. Soukoulis (Kluwer, Academic, Dordrecht, 2001).

[20] M. Notomi, Phys. Rev. B **62**, 10 696 (2000).